Predicting Emergence of Nanoscale Order in Surface Oxides through Preferential Interactivity Parameter

Andrew Martin,[1] Martin M. Thuo[1,*]

[1] North Carolina State University, Department of Materials Science and Engineering. Raleigh, NC 27695. USA

*Corresponding author: mthuo@ncsu.edu

KEYWORDS Interfacial engineering, oxidation, surface science, metal oxides, mass transport

ABSTRACT: Diffusion and surface oxidation are critical, and necessary, processes in metal alloy designs and use. Surface oxide provides unique opportunities to improve material properties or performance beyond bulk alterations. Surface oxidation is, however, often oversimplified into a classical diffusion process. Passivating oxide surfaces are also thought to be lacking in complexity or critical information. A closer look, however, shows inherent complexity with kinetics-driven competition between the elements in the process leading to redox-speciation across a very small (nm) thickness. Questions that remain to be answered for a comprehensive understanding of surface oxides are diverse and call for interdisciplinary approaches. By using thermodynamics-based preferential Interactivity Parameter (PIP) alongside kinetic consideration, we show how complexity in these oxides can be predicted allowing us to tailor these thin films. We use our work and that of others to illustrate predictability while also highlighting that there is still much more to be done.

At ambient conditions, surface oxides are critical inherent nanocomponents of metal alloys but their understanding and/or effect on the bulk is an ongoing study. This small nano-scale component[1] is either sought after to enhance material properties through interfacial engineering or deemed a menace as they generate unwanted chemistries/reactions,[2] alter surface properties, or introduce defects (most notable in corrosion science).[3] Many theories have given us better understanding towards the kinetics of oxidation,[4-6] providing critical information on rates, morphology, and organization of these oxides from early to later stages. Understanding the coupling between intrinsic elemental properties with external forces is, however, still highly limited. Exploring this problem inevitably requires expansion of our viewpoint beyond classical mechanics and unary stimuli effects. Current miscibility and diffusion rules[7-10] for predicting inter-diffusion in a mixture apply correlations between elements hence are inherently limited as they fail to consider asymmetry in interactions along the diffusion path especially in multicomponent alloys.[11] Oxidizing alloys, however, have co-dependent interactions between diffusing elements that drive the overall flux (J_{tot}) from early (entropy dependent) to late (distance, path, and mobility dependent) stages of oxidation (Figure 1a). This interdependency forces us to consider that flux of individual element (J_i) and their thermodynamic potentials ($\nabla\phi_i$) have influence on others. For example, at the initial stage (single atom layer), principle of equal *apriori* probabilities dictates that solid and liquids would oxidize similarly since there is limited diffusion (Figure 1a). As the oxide layer grows to several nm thick, diffusion through the statistical stoichiometry-dictated layer becomes critical in defining progress or passivation. At higher thicknesses, the mechanism between a solid and a liquid diverges given differences in surface elasticity and plasticity of the two (Figure 1a).[12] Given the importance of this nm thick oxide in surface oxidation, are surface oxides studies purely nanoscience? Or should the community pay more attention given the significant effect of surface oxides in the economy and in controlling material properties? This perspective shows the need to rethink surface oxides and reactions from a nanoscience view given that it is not just the top layer of atoms that matter but also the underlying sub-surface (nm) reconstruction. Both of which are of great interest for the scientific community and have a major role to play in corrosion, surface treatment and related processes.

Herein, we present oxidation as a predominantly multi-tensor dictated flux and reaction, in part due to preferential interactions (hence a dictated

diffusion path) and stoichiometric interdependency on which element oxidizes and at what stage of the process it does. Classical definition of oxidation couples the flux with forces from a concentration gradient, herein we explore other contributing factors (e.g., surface plasticity above) that dictate differences in oxides or passivating layers in metals.

For brevity and clarity, we apply the so-called Preferential Interactivity Parameter (PIP) as a basic, simple, thermodynamics guiding tool to explain literature data and highlight why nanoscience tools are critically needed in this field (Figure 1b).[13] The PIP utilizes a three axis plot to capture the push (Standard reduction potential, E^0),[14] pull (Cohesive energy density, CED),[15] and barrier (covalent radius/size, r)[16] to an element's ability to diffuse towards a reaction (in this case oxidation) front. The E^0 captures propensity to oxidize hence a thermodynamic 'push' of the metal atoms towards the oxidant or of the oxidant towards the element. Here, E^0 values are relative to a standard hydrogen electrode and are used as obtained from literature. Covalent radius captures the size-dependent barrier to diffusivity as dictated by classical mechanics. The CED captures energy cost to 'escape' from an initial state or bound environment into an atomized state, hence it captures the 'pull' for an element against diffusion towards the reaction front. For brevity, we use CED to capture displacement energy of an elements from its bulk (which indirectly encompasses bond strength, lattice/structure mismatches, and miscibility). This static view aligns well with thermodynamics but under kinetic consideration, it would evolve with the changing environment hence more theoretical work is needed. Given that surface oxidation deals with atomic migration from the bulk, we consider CED captures 'inertia' – resistant to escape an initial state. Standard reduction potential (here given relative to NHE), E^0, on the other hand, captures propensity to oxidized, albeit in the reverse direction. In a simplified way, E^0 captures ease of accessibility to oxidation pathways in a thermodynamic energy landscape. Reduction potential is used here *in lieu* of electronegativity that waspreviously applied in miscibility rules (Hume-Rothery rules, Chelikowsky plots, and Gordy-Thomas equations)[7, 17-20] as it is readily referenced and well defined.- Covalent radius, r, captures effect of an elements size in diffusion akin to that defined by the Stokes–Einstein–Sutherland equation ($D\alpha 1/r$). This is under the assumption that the element is not charged, otherwise a correction (based on charge density) should be made as atomic drift velocity instead of random walk dominates flux. . It has also been shown that differences in atomic size affects surface-bulk favorability and ability to fill interstitial gaps that form during oxidation.[21] For clarity and brevity in the 3D plot, these parameter can be presented on a log scale. Mapping these properties in tandem establishes a ranking order and helps predict how a surface reaction (oxidation) occurs and associated surface speciation. While PIP can help guide initial predictions of surface preference and organization, oxidation depends on other variables (e.g., phase, external factors, stoichiometry, entropic contribution, etc.), that this perspective aims to explore (Figure 1).

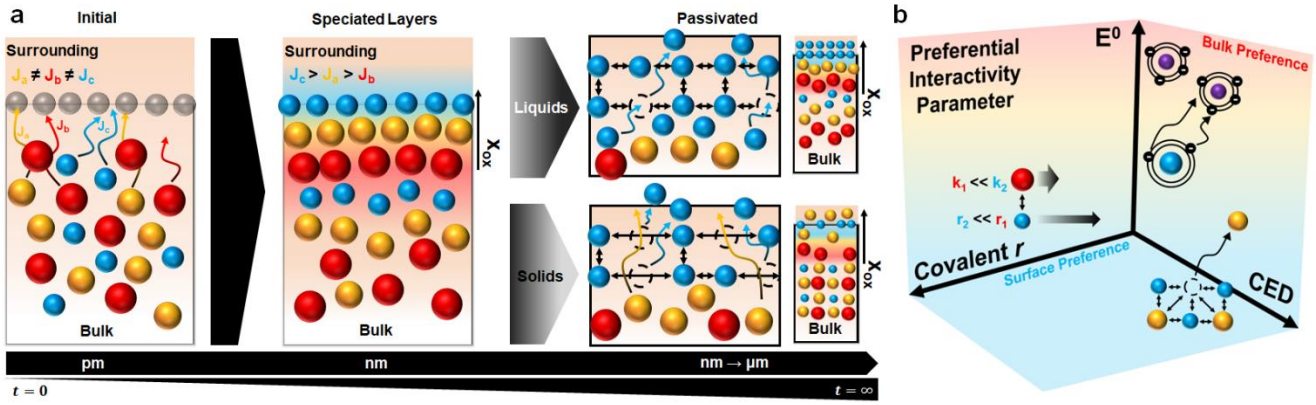

Figure 1. (a) Schematic of oxidation conditions for multi-element alloy system from its native state to extended oxidation stage, where blue>yellow>red indicates atoms with highest to lowest diffusivity. Bulk phase (liquid or solid) dependent differences in surface distribution/organization of elements on extended oxidation (b) General schematic of the Preferential Interaction Parameter. Legends: radius; red>yellow>blue. For E^0, blue<yellow<red for the metalalloy components, purple = oxygen .

Oxidation Stages and Phases

In the initial (oxidation time, t=0) oxide formation stage (Figure 1a), all surface atoms (grey) of a hypothetical alloy oxidize in a stoichiometrically-limited statistical manner (principle of equal *a priori* probabilities). Depending on the different reacting elements, however, the flux of these different species is not equal ($J_a \neq J_b \neq J_c$) hence a differentiation ensues at t>0 during the oxidation process. This early stage is primarily dominated by entropy and statistical mechanics where the highest probability to form the surface oxide is not dependent on their position within the PIP. Once the reaction initiates and the a prior surface elements are consumed, oxidation will depend on an elements position in the 3D plot (Figure 1b, low r, low CED, and low E^0). Element that has a higher propensity to partition to the surface (blue zone) dominates initial oxide layer with concomitant segregation of the statistically reacted components right below this initial layer.After the initial oxide layer forms, the oxidizing front migrates either inward (oxidant diffuse in) or outward (metal atoms diffuse out). In the latter, surface oxidation is dependent on the distance that atoms must travel, i.e. thickness of the oxide ($\partial c/\partial x$) alongside interaction with other alloy elements. Increasing oxide thickness alters the mobility ($c_i M_i$) and exchange probabilities for both oxygen anions and metal cations with regimes dictated by the size of the oxide (Figure 1a). Oxidation can therefore be viewed as a two-stage process; i) early (a few nm thick) and ii) late stages (more than tens of nm thick), with a likely intermediate state. Given the thickness and changes in diffusivity, these regimes can be defined based on underlying kinetic relations. The two stages are Cabrera-Mott (inverse logarithmic type rate law) and Wagner (parabolic growth rate law) regimes, with an intermediate so-called XRB (direct logarithmic rate law) regime.[4-6] Increase in thickness not only alters the underlying rate law, but also induces phase change in the surface oxide layer. In the Cabrerra-Mott regime, surface oxides are pliable nanolayers and likely not fully crystalline. In the Wagner regime, however, the surface oxide is mechanically rigid and brittle akin to the bulk analog.[12] Considering liquid metals, redox-dictated speciation dominate early stages while fractures in the brittle thicker oxide may allow for the speciated components to diffuse out (especially if the bulk is a liquid under pressure), leading to composition inversion and texture modification.[22-23] Surface elastic deformation in solids, however, implies that although speciation occurs in the early stages, fractures in thicker oxides would allow for rapid oxidant diffusion presenting low E^0 oxides deeper into the surface albeit with a fracture on top of them. Given these differences and for clarity, we separate the ensuing discussion into liquid and solid metals.

Liquids

Previously, we employed PIP to predict the oxidation behavior of liquid metals.[22-24] Utilizing standard reduction potential (E^0), covalent radius and cohesive energy density (CED) as the guide for propensity to localization on the surface hence oxidize (blue) while also capturing miscibility, a key factor in understanding early sub-oxide formation and speciation (Figure 2a). When elements are well mixed, the initial statistical thermodynamics-dictated process stoichiometrically presents all elements. Where the metal is eutectic (uniform liquid) , elements inside the miscibility sphere are randomly (statistical probability) presented to the surface. Various studies have been carried out to understand surface oxides in liquid metals.[25-29] Angle resolved x-ray photoelectron spectroscopy (ARXPS) and time-of-flight secondary ion mass spectrometry (TOF-SIMS) confirmed the PIP predicted speciation in a binary eutectic gallium indium (eGaIn).[2, 29-30] The depth profile displays a speciation behavior with Ga_2O_3 as the primary oxide ($E^0_{Ga} = -0.56V$, $CED_{Ga} = 0.01\ Pa$) [14-16] dominating the outer oxide albeit with a gradient in oxidation state with increase in depth. Suboxides of In ($E^0_{In} = -0.34V$, $CED_{In} = 47.6\ Pa$) [14-16] are also found deeper in the oxide, capturing the validity of the principle of equal *apriori* probability. The order in oxidation states induces a surface dipole that is compensated by segregation of pure Ga then In metals below the oxide to form a transition layer from the oxide to the bulk eutectic (Figure 2b). We inferred that growing the oxide layer should increase the speciated material. This was confirmed through thermo-oxidative composition inversion (TOCI),[22-24] where a particle of the liquid metal is heated at low oxygen allowing the oxides to slowly thicken.

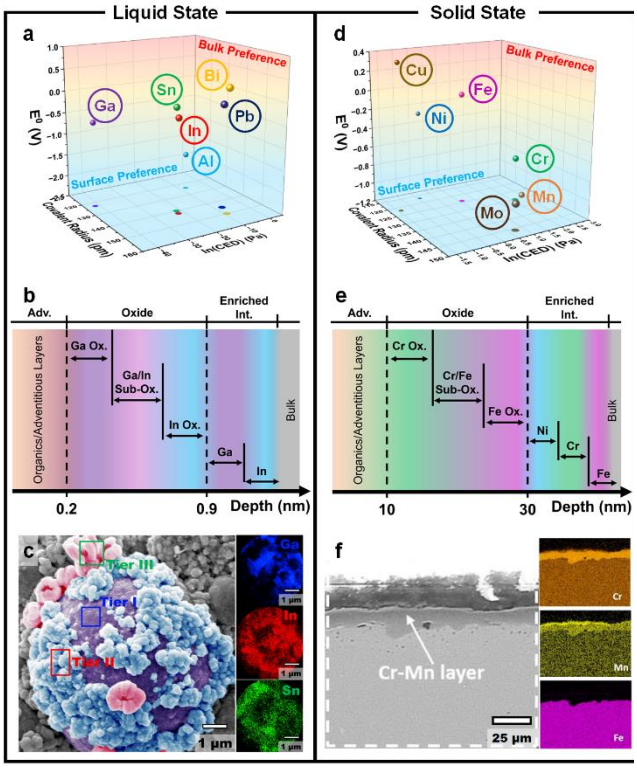

Figure 2. Analysis of oxidation in liquid and solid alloys. (a) PIP for common liquid/soft metals. (b) Depth profile of EGaIn at ambient condition. (c) SEM image and EDX map of GaInSn oxidized at 900°C for 1 hr. Map legends: Ga = blue, In = red and Sn = green. Reproduced with permission from reference 23. Copyright 2020 Wiley Publishing. (d) PIP for common steel alloy components. (e) Depth profile of oxidized AISI-304 steel (FeCrNi). (f) STEM-EDX map of FeCrMn alloy oxidized at 1000°C for 100 hrs. Map legends: Cr = orange, Mn = yellow and Fe = purple. Reproduced with permission from reference 34. Copyright 2021 Elsevier.

With continued heating, the liquid metal continues to expand while the oxide gets more rigid hence pressure builds up. Eventually, the oxide fractures sequentially releasing the pressurized sub-layers that then oxidize to form an oxide layer whose composition is opposite of the oxidizing liquid. Figure 2c shows the inversion of GaInSn. Empirical observation of unprecedented oxides under TOCI confirmed the spectroscopic data, illustrating that predictions from PIP can be used to understand other alloy systems. We, however, also note that during oxidation of metastable metal particles, the progression from Cabrerra-Mott to Wagner regime is rapid, suggesting that PIP is a good tool for predictions related to equilibrated systems. Far from equilibrium systems may require a recalibration of the terms and is work in progress.

Solids

The most straightforward example of oxide passivation in solid metal alloy is in stainless steel (AISI 304) and other iron-chromium alloys.[31-33] The fundamental idea that was used to create a corrosion-resistant iron-based alloy involves the addition of chromium ($E^0_{Cr} = -0.74\,V$, $CED_{Cr} = 8.24\,Pa$), an element with significantly higher propensity to oxidize compared to iron ($E^0_{Fe} = -0.04\,V$, $CED_{Fe} = 1.81\,Pa$).[14-16] This alloy design was employed with the specific aim of passivating bulk iron, hence, resist long-term corrosion. Using PIP, (Figure 2d) we can predict elements that have moderate miscibility to Fe but have high preference for the surface. Elements such as Cr or Mn would dominate the surface of steel hence are good passivating agents. Despite the low concentration of Cr in stainless steel ($c_{Cr} = 0.18$ vs. $c_{Fe} = 0.74$), Cr_2O_3 still dominates the surface (Figure 2e).[31-32] Similarly, when Mn is added into the system ($E^0_{Mn} = -1.18V$, $CED_{Mn} = 11.6\,Pa$) a change in the passivation order can be seen where Mn now dominates the surface as $PIP_{Mn} < PIP_{Cr}$ (Figure 2f).[34]

These examples (in both liquids and solids) are simple examples of how mapping combinations of elements within a parametric space can assist us in predicting compositional gradient in dissipative events (such as oxidation or self-assembly/speciation). In summary, PIP can predict speciation behavior in both liquid and solid systems, albeit at different time and dimensional scales. Liquid systems sit far from equilibrium with minimum diffusion lengths (<1 nm), thus reaction kinetics are enhanced even at ambient conditions. Formation of speciated regions are rapid and often not noticeable due to its scale and difficulty to characterize (several atoms thick in its native condition).[22, 29-30] TOCI provides a pathway to characterize these regions through extended oxidation and growth, transforming a liquid-like oxide (Cabrera-Mott) into a semi-solid (Wagner) where observation can be more readily made, albeit in an inverted condition. Nonetheless, this methodology demonstrates Shuttleworth's theorem[12] on surface deformation differences between liquids and solids. Equilibrated solids provide a snapshot of a later stage oxidation that can be pushed to further reactions. We understand that these speciation events span beyond traditional kinetic parameters (diffusion coefficient, heat capacity, conductivity) and involve multiple extrinsic factors that cannot be captured in a static plot, especially in the extended stage. We here

analyzed data derived from different conditions with PIP as a guide to assess its validity.

Reaction Conditions and Stoichiometry

Switching the scope to a different system, we generated PIP for Ti-based refractory alloys (Figure 3a). Here, we explore the role of atmospheric conditions during oxidation as one of the driving forces in the diffusion/speciation process. Given the symmetry in oxidation and reduction, E^0 bears a negative sign under oxidation but is positive under reducing conditions. Examining TaTiCr as an example, Ti has the highest E^0 value ($E^0_{Ti} = -0.16V$ vs $E^0_{Cr} = -0.74\,V$ and $E^0_{Ta} = -0.75\,V$). Under an oxidizing environment Ta or Cr are expected to dominate the surface, with Ti buried in the subsurface unless under TOCI. Figure 3b shows a Ti-Cr-Ta order in the surface oxides showing that the oxidation was run for an extended period or under reducing conditions, since this order is inverse of the redox values.[35] The reducing environment is ascertained by subsurface nitrogen enrichment from the oxidation methodology.[35]

Given the stochastic nature (probabilistic atomic collisions) of the surface reaction, we infer that stoichiometry should play a major role. In TaTiCr, all elements are equimolar, hence surface speciation can be thermodynamically (PIP) predicted. In Ta_4TiCr_3 (4:1:3 Ta:Ti:Cr molar ratio), Ta dominates the surface oxide with no detectable amounts of Ti (Figure 3c). We infer that this is stoichiometry driven given the low concentration of Ti in the bulk. From PIP (Figure 3a) surface oxidation of these refractory alloy is dominated by Ta unless an element with a lower E^0 value is added (Commonly Al, $E^0_{Al} = -1.66V$).[36-37] Given that statistics/probability as manifested in stoichiometry play a role in the nature of these surface oxides, we inferred that PIP could also help our understanding of oxidation in high entropy alloys (HEA).

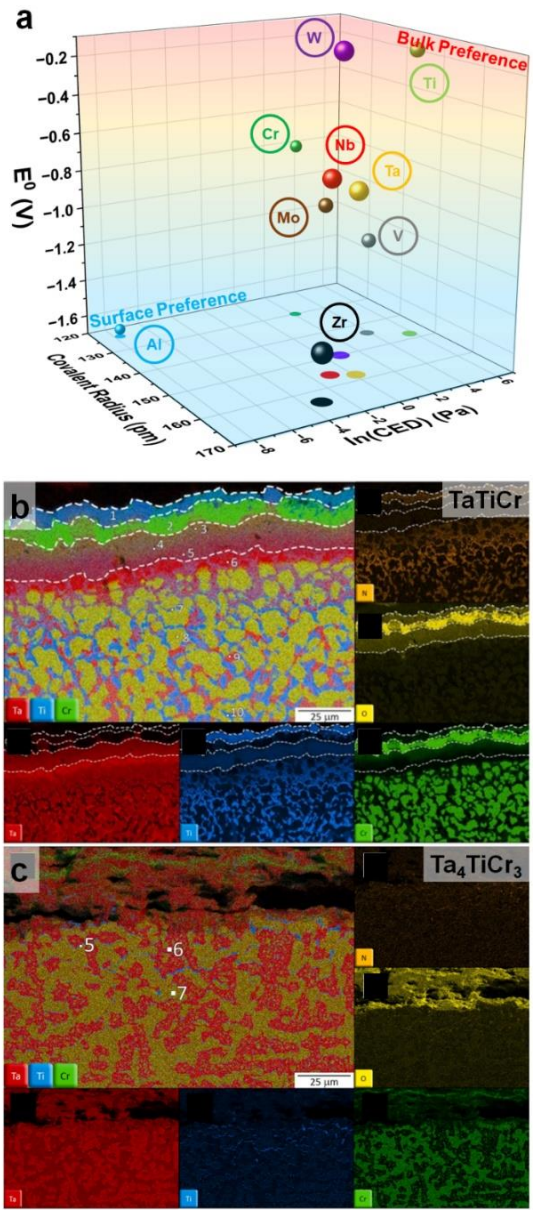

Figure 3. Analysis of oxidation in refractory alloys. (a) PIP for common refractory alloy elements. (b) STEM-EDX map of TaTiCr alloy oxidized at 1200°C for 24 hrs. Reproduced with permission from reference 35. Copyright 2023 Elsevier. (c) STEM-EDX map of Ta_4TiCr_3 alloy oxidized at 1200°C for 24 hrs. Map legends: N = orange, O = yellow, Ta = red, Ti = blue and Cr = green. Reproduced with permission from reference 35. Copyright 2023 Elsevier.

Role of Composition Entropy

We take PIP further into high entropy systems with ≥ 4 principal elements (Figure 4a) and analyze an equimolar HEA, CrMnFeNi[38] or CrMnFeNiCo.[39] This alloy has recently surged in interest due to its improved strength, ductility and strain hardenability.[40-41] The presence of many (n_i, $i \geq 4$) interacting species within a system, however, has significant effects towards diffusion (akin to colligative property) since inter-element interactions can be either

enhancing or disruptive. High entropy, however, should create a system where the highest statistically probable event dominates. Given these elements are widely different in the PIP plot, we can divide these groupings into fast (Mn and Cr) and slow (Fe and Ni) oxidizing elements. Figure 4b[38-39] shows a surface dominated by Mn > Cr, similar to Figure 2f. Domination by Mn follows our thermodynamic prediction from PIP as $PIP_{Mn} < PIP_{Cr}$. Similar system with different oxidizing condition have also revealed the presence of small Fe oxide island on the surface layer,[39, 42] indicating that within this solid system at an extended stage, slow oxidizing elements have the probability to diffuse through defects akin to TOCI (Figure 1a). It is therefore important that one does not apply PIP, a thermodynamic parameter, without consideration of kinetics especially under the presence of extended stimuli.[43]

Relation to Other Models

In comparison to other oxidation models, where detailed kinetic and transport event are reconstructed either through Monte Carlo simulations, Finite Element Analysis, or more recently AI-assisted machine learning algorithms,[44-47] PIP provides its benefit in its simplicity through statistical probability and thermodynamic basis. PIP operates at different timescale compared to other live models. Currently, PIP defines its prediction through coupling of different thermodynamic factors without considerations of extended kinetics aspect. Whilst PIP is limited in predicting formed structure, long-term stability, or in-situ placements of different atomic species overtime, PIP excels in statistically predicting order and speciation. We believe that PIP can serve as a beneficial supplement to these kinetic models by laying down the initial hypothesis and prediction of any given system due to its modularity. As an ongoing work, we continue to monitor these new works in effort to i) further confirm the feasibility of PIP under different systems and ii) improve the accuracy of PIP where necessary.

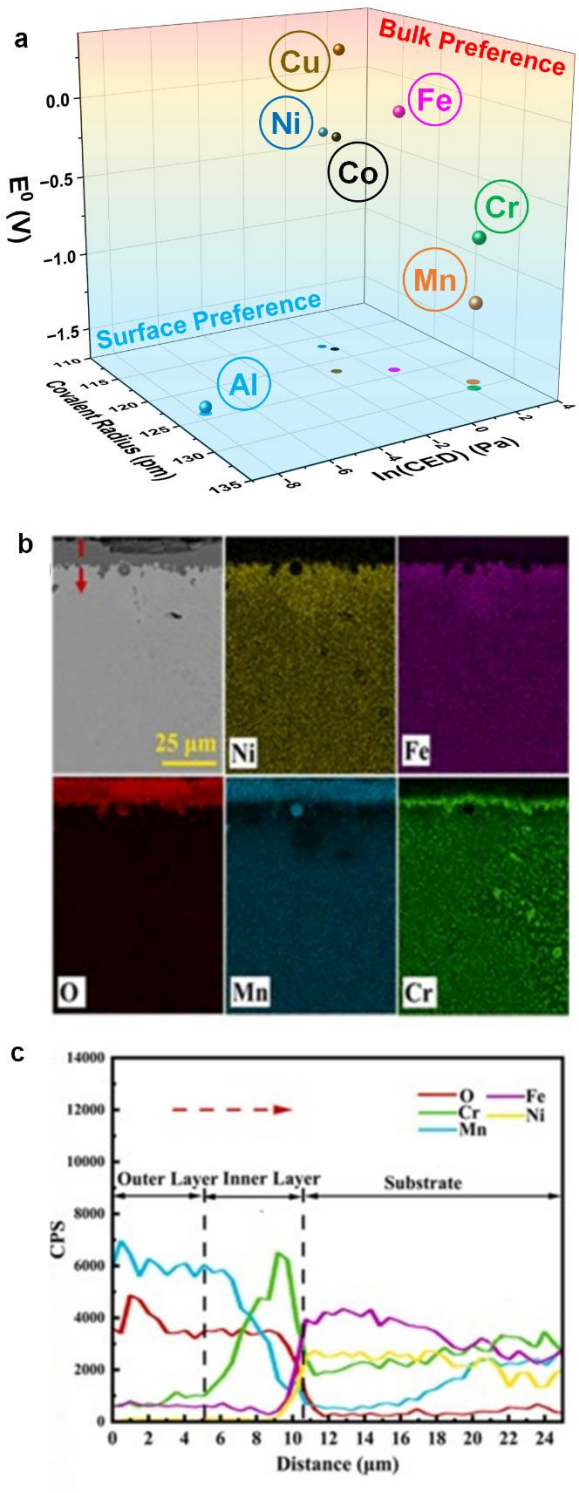

Figure 4. Understanding oxidation and speciation in High Entropy Alloys (HEA) (a) PIP with common elements within HEA. (b) STEM-EDX map for CrMnFeNi alloy oxidized at 800°C for 108 hrs in air. Map legends: Ni = yellow, Fe = purple, O = red, Mn = blue and Cr = green. (c) EDX depth profile of the sample shown in b. red arrow indicates region of interest. Reproduced with permission from reference 38. Copyright 2022 Elsevier.

Perspective and Future Work

Despite the agreement of PIP plots to experiments, there is still a lot more to explore to fully

realize its utility, but more interestingly to encourage the nanoscience community to investigate these consequential nanolayers on bulk materials. Studies on CED values for elements precipitated in presence of miscible participants, may be different than in the pure element. Does this relate to thermodynamic stability of the crystal structure? For example, Ni is commonly used as a phase stabilizer due to its high structural energetic barrier ($E_{BCC} \gg E_{FCC}$). Is this fully captured in the CED or is interaction with adjacent element affecting diffusivity leading to frustrated diffusion? If we do capture all of these parameters, however, we simply cannot fit them in a 2-dimensional landscape, which calls for a higher dimension perspective on the thermodynamic energy landscape.

Whilst PIP can be utilized to better our thermodynamic understanding in mixed multi-elemental systems, this parameter is still in its infancy and requires more empirical data. To which, it requires scientists from different disciplines (not only metallurgists, but also nano scientists, chemists, physicists, etc.) to expose the rough edges. While all the examples shown above utilized absolute value taken from handbooks and database,[14-16] we have since considered that due to the interdependency of different elements in a mixed material system, PIP might have better representation as a relative function (Figure 5a). Figure 5 is a normalized PIP of period 4 transition metals, from which we can see their miscibility and surface/bulk preferences. From this normalized parameter, we see why Fe and Ni are miscible with many of these elements, hence, they are commonly used as alloying host/component (for superalloys/steels).[40, 48-49] The PIP properties (E^0, CED and size) of Ni and Fe place this element close to the center of this series hence, they can readily envelop most others within the 10%:10%:15% (E^0:CED:radius) miscibility envelop as the bubbles in the plot indicate. This prediction captures the initial miscibility conditions and may evolve as the system undergoes different oxidation conditions.

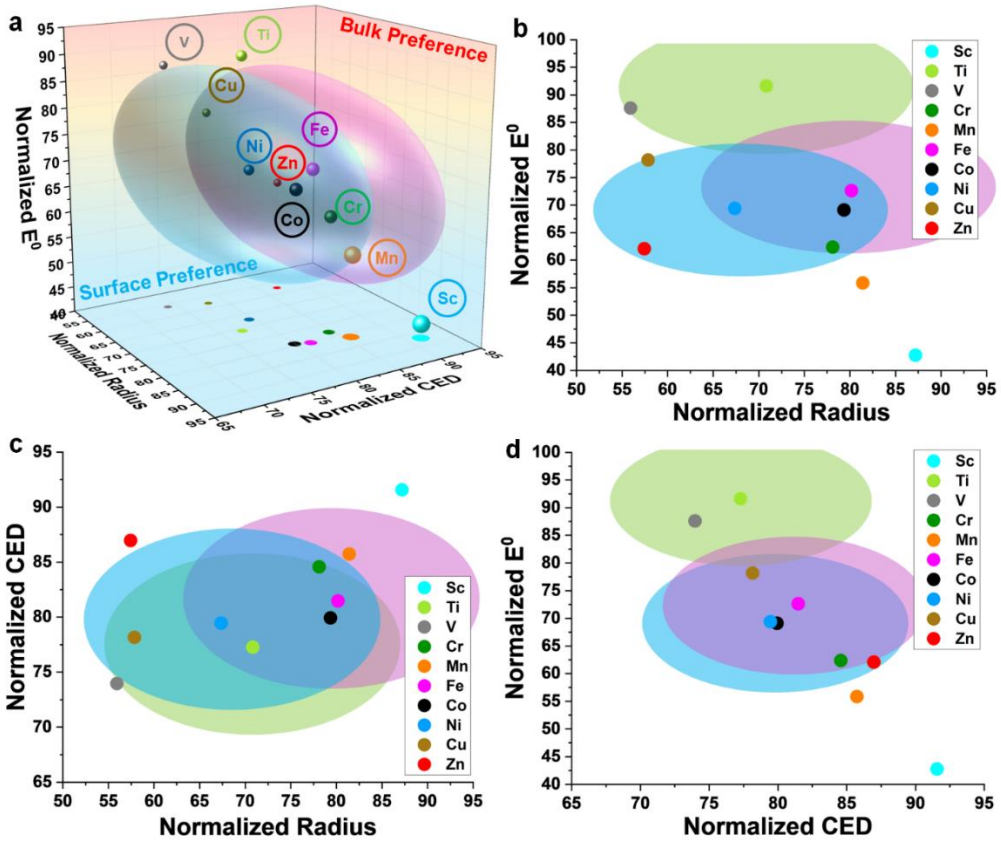

Figure 5. Normalized PIP and its 2-dimensional views. (a) Normalized PIP for period 4 transition metals. Where the bubble indicates miscibility window. (b-d) 2-dimensional view of correlation between E^0-radius, CED-radius and E^0-CED respectively.

Beyond the 3-dimensional view of PIP, some may still find benefits from utilizing it in a 2-dimensional scale, such as between E^0 and radius akin to Darken-Gurry plots (Figure 5b).[18, 50] From these 2-

dimensional views of PIP (Figure 5b-d), one can determine which property is more dominating in a mixed-element system. Some elements are more generally compatible with different elements (such as Fe and Ni above), whilst others (e.g., Ti) may only be compatible under different conditions. It can also be easily seen why Sc is not a common alloying element to its period 4 neighbors likely due to miscibility challenges with its PIP properties far removed from all the others, although it can potentially dominate the surface oxide and be a compatible passivating material.[14-16] It is well understood that the thermodynamic energy landscape can be transformable under different conditions and thus systems beyond the prediction of PIP may be created. Hence, it is advised to take the interpretation of PIP with kinetic considerations.

Given all the examples shown here from us and independently by others, we infer that surface oxidation of metals entails complex nanoscience. We, however, highly limit ourselves by creating generalized assumptions and viewing oxidation as a classical thermodynamic phenomenon, even though diffusion/diffusivity plays a critical role. Perturbation of diffusion by inter-atomic interaction extends it into the quantum regime since these interactions lead to distortion of valence electrons and the associated Cyrot-Lackmann binding energy. Similarly, borrowing from the Einstein-Smoluchowski equation,[51] current diffusion model lacks the interdependency of multiple interacting stressors and role of external factors that may help accurately represent oxidation. Expanding our viewpoint beyond a linear classical thermodynamic system is a requirement in order to achieve said goal. In conclusion, there are still more work to be done and science to be unveiled within this nano-scale phenomenon.

AUTHOR INFORMATION

Corresponding Author

*Martin Thuo, mthuo@ncsu.edu

Author Contributions

The manuscript was written through contributions of all authors.

ACKNOWLEDGEMENTS

This work was supported by North Carolina State University startup funds and by the National Science Foundation under Award No. 2243104.

REFERENCES

1. Martin, A.; Chang, B. S.; Pauls, A. M.; Du, C.; Thuo, M. M., Stabilization of Undercooled Metals via Passivating Oxide Layers. *Angew. Chem. Int. Ed.* **2020,** *60* (11), 5928-5935.
2. Hsieh, T.-E.; Frisch, J.; Wilks, R. G.; Bär, M., Unravelling the Surface Oxidation-Induced Evolution of the Electronic Structure of Gallium. *ACS Appl. Mater. Interfaces* **2023,** *15* (40), 47725-47732.
3. West, J. M., *Basic corrosion and oxidation. Second edition*. John Wiley and Sons Inc.,New York, NY: United States, 1986.
4. Cabrera, N.; Mott, N. F., Theory of the oxidation of metals. *Rep. Prog. Phys.* **1949,** *12* (1), 163-184.
5. Xu, Z.; Rosso, K. M.; Bruemmer, S., Metal oxidation kinetics and the transition from thin to thick films. *Phys. Chem. Chem. Phys.* **2012,** *14* (42), 14534-14539.
6. Atkinson, A., Wagner theory and short circuit diffusion. *Mater. Sci. Technol.* **1988,** *4* (12), 1046-1051.
7. Hume-Rothery, W., Research on the Nature, Properties and Conditions of Formation of Intermetallic Compounds, with Special Reference to Certain Compounds of Tin. *J. Inst. Metals* **1926,** *35*, 295-361.
8. Clendinnen, F. W. J.; Rivett, A. C. D., CLII.—The ternary system ammonium chloride–manganous chloride–water. *J. Chem. Soc. Trans.* **1921,** *119* (0), 1329-1339.
9. Gschneidner Jr., K. A.; Verkade, M., Electronic and crystal structures, size (ECS²) model for predicting binary solid solutions. *Prog. Mat. Sci.* **2004,** *49* (3), 411-428.
10. Waber, J. T.; Gschneidner, K., Jr.; Larson, A. C.; Prince, M. Y., Prediction of Solid Solubility in Metallic Alloys. *Trans. Metall. Soc.* **1962,** *227*, 717.
11. Martin, A.; Thuo, M., Beyond Hume-Rothery Rules. *Acct. Mater. Res.* **2023**.
12. Shuttleworth, R., The Surface Tension of Solids. *Proc. Phys. Soc., London, Sect. A* **1950,** *63* (5), 444.
13. Martin, A.; Chang, B. S.; Thuo, M., Effect of Surface Nanostructures and Speciation on Undercooling for Low-Temperature Solder Alloys. *ACS Appl. Nano Mater.* **2022,** *5* (3), 3325-3332.
14. Vanýsek, P., Electrochemical Series. In *CRC Handbook of Chemistry and Physics, 95th Edition*, Haynes, W. M., Ed. CRC Press: Hoboken, NJ, 2014; pp 5-80.
15. Yaws, C. L.; Satyro, M. A., Chapter 2 - Vapor Pressure – Inorganic Compounds. In *The Yaws Handbook of Vapor Pressure (Second Edition)*, Yaws, C. L., Ed. Gulf Professional Publishing: 2015; pp 315-322.
16. Mantina, M.; Valero, R.; Cramer, C. J.; Truhlar, D. G., Atomic Radii of The Elements. In *CRC Handbook of Chemistry and Physics, 95th Edition*, Haynes, W. M., Ed. CRC Press: Hoboken, NJ, 2014; pp 9-49.
17. Martin, A.; Thuo, M., Beyond Hume-Rothery Rules. *Acct. Mater. Res.* **2023,** *4* (10), 809-813.
18. Mae, Y., What the Darken–Gurry Plot Means About the Solubility of Elements in Metals. *Metall. Mat. Trans. A* **2016,** *47* (12), 6498-6506.
19. Chelikowsky, J. R., Solid solubilities in divalent alloys. *Phys. Rev. B* **1979,** *19* (2), 686-701.
20. Gordy, W.; Thomas, W. J. O., Electronegativities of the Elements. *J. Chem. Phys.* **2004,** *24* (2), 439-444.
21. Wang, L.-L.; Johnson, D. D., Predicted Trends of Core–Shell Preferences for 132 Late Transition-Metal Binary-Alloy Nanoparticles. *J. Am. Chem. Soc.* **2009,** *131* (39), 14023-14029.
22. Cutinho, J.; Chang, B. S.; Oyola-Reynoso, S.; Chen, J.; Akhter, S. S.; Tevis, I. D.; Bello, N. J.; Martin, A.; Foster, M. C.; Thuo, M. M., Autonomous Thermal-Oxidative Composition Inversion and Texture Tuning of Liquid Metal Surfaces. *ACS Nano* **2018,** *12* (5), 4744-4753.
23. Martin, A.; Kiarie, W.; Chang, B.; Thuo, M., Chameleon Metals: Autonomous Nano-Texturing and Composition Inversion on Liquid Metals Surfaces. *Angew. Chem. Int. Ed.* **2020,** *59* (1), 352-357.
24. Martin, A.; Chang, B.; Cutinho, J.; Shen, L.; Ward, T.; Cochran, E. W.; Thuo, M. M., Passivation-driven speciation, dealloying and purification. *Mater. Horiz.* **2021,** *8* (3), 925-931.

25. Regan, M. J.; Tostmann, H.; Pershan, P. S.; Magnussen, O. M.; DiMasi, E.; Ocko, B. M.; Deutsch, M., X-ray study of the oxidation of liquid-gallium surfaces. *Phys. Rev. B* **1997,** *55* (16), 10786-10790.
26. Tostmann, H.; DiMasi, E.; Pershan, P. S.; Ocko, B. M.; Shpyrko, O. G.; Deutsch, M., Surface structure of liquid metals and the effect of capillary waves: X-ray studies on liquid indium. *Phys. Rev. B* **1999,** *59* (2), 783-791.
27. Scharmann, F.; Cherkashinin, G.; Breternitz, V.; Knedlik, C.; Hartung, G.; Weber, T.; Schaefer, J. A., Viscosity effect on GaInSn studied by XPS. *Surf. Interface Anal.* **2004,** *36* (8), 981-985.
28. Dumke, M. F.; Tombrello, T. A.; Weller, R. A.; Housley, R. M.; Cirlin, E. H., Sputtering of the gallium-indium eutectic alloy in the liquid phase. *Surf. Sci.* **1983,** *124* (2), 407-422.
29. Cademartiri, L.; Thuo, M. M.; Nijhuis, C. A.; Reus, W. F.; Tricard, S.; Barber, J. R.; Sodhi, R. N. S.; Brodersen, P.; Kim, C.; Chiechi, R. C.; Whitesides, G. M., Electrical Resistance of Ag^{TS}-$S(CH_2)_{n-1}CH_3$//Ga_2O_3/EGaIn Tunneling Junctions. *J. Phys. Chem. C* **2012,** *116* (20), 10848.
30. Sodhi, R. N. S.; Brodersen, P.; Cademartiri, L.; Thuo, M.; Nijhuis, C. A., Surface and buried interface layer studies on challenging structures as studied by ARXPS. *Surf. Interface Anal.* **2017,** *49* (13), 1309-1315.
31. Greyling, C. J.; Roux, J. P., Optimum conditions in the thermal passivation of aisi 430 and 304 stainless steel in controlled oxygen atmosphere. *Corros. Sci.* **1984,** *24* (8), 675-690.
32. Greeff, A. P.; Louw, C. W.; Swart, H. C., The oxidation of industrial FeCrMo steel. *Corros. Sci.* **2000,** *42* (10), 1725-1740.
33. Tjong, S. C.; Eldridge, J.; Hoffman, R. W., EAS studies of the oxides formed on iron-chromium alloys at 400°C. *Appl. Surf. Sci.* **1983,** *14* (3), 297-306.
34. Zhan, J.; Yang, Y.; Bi, H.; Li, M.; Gu, H., High temperature oxidation behavior of type 444 stainless steel in synthetic automotive exhaust gas. *J. Mater. Res. Technol.* **2021,** *12*, 530-541.
35. Welch, N. J.; Quintana, M. J.; Butler, T. M.; Collins, P. C., High-temperature oxidation behavior of TaTiCr, Ta_4Ti_3Cr, Ta_2TiCr, and Ta_4TiCr_3 concentrated refractory alloys. *J. Alloys Compd.* **2023,** *941*, 169000.
36. Ostovari Moghaddam, A.; Sudarikov, M.; Shaburova, N.; Zherebtsov, D.; Zhivulin, V.; Ashurali Solizoda, I.; Starikov, A.; Veselkov, S.; Samoilova, O.; Trofimov, E., High temperature oxidation resistance of W-containing high entropy alloys. *J. Alloys Compd.* **2022,** *897*, 162733.
37. Lo, K.-C.; Chang, Y.-J.; Murakami, H.; Yeh, J.-W.; Yeh, A.-C., An oxidation resistant refractory high entropy alloy protected by $CrTaO_4$-based oxide. *Sci. Rep.* **2019,** *9* (1), 7266.
38. Zhang, Y.; Wu, H.; Yu, X.; Tang, D., Role of Cr in the high-temperature oxidation behavior of CrxMnFeNi high-entropy alloys at 800 °C in air. *Corros. Sci.* **2022,** *200*, 110211.
39. Holcomb, G. R.; Tylczak, J.; Carney, C., Oxidation of CoCrFeMnNi High Entropy Alloys. *JOM* **2015,** *67* (10), 2326-2339.
40. Miracle, D. B.; Senkov, O. N., A critical review of high entropy alloys and related concepts. *Acta Mat.* **2017,** *122*, 448-511.
41. Pickering, E. J.; Jones, N. G., High-entropy alloys: a critical assessment of their founding principles and future prospects. *Int. Mater. Rev.* **2016,** *61* (3), 183-202.
42. Gwalani, B.; Martin, A.; Kautz, E.; Lambeets, S.; Olszta, M.; Battu, A.; Malakar, A.; Yang, F.; Guo, J.; Thevuthasan, S.; Thuo, M.; Devaraj, A., Mechanistic Understanding of Speciated Oxide Growth in High Entropy Alloys PREPRINT (Version 1). *available at Research Square* **2023**.
43. Martin, A.; Pauls, A. M.; Chang, B.; Boyce, E.; Thuo, M., Photo-Activated Growth and Metastable Phase Transition in Metallic Solid Solutions. *Adv. Mater.* **2023,** *n/a* (n/a), 2309865.
44. Du, X.; Damewood, J. K.; Lunger, J. R.; Millan, R.; Yildiz, B.; Li, L.; Gómez-Bombarelli, R., Machine-learning-accelerated simulations to enable automatic surface reconstruction. *Nat. Comput. Sci.* **2023,** *3* (12), 1034-1044.
45. Wang, W.; Chen, S.; Pei, C.; Luo, R.; Sun, J.; Song, H.; Sun, G.; Wang, X.; Zhao, Z.-J.; Gong, J., Tandem propane dehydrogenation and surface oxidation catalysts for selective propylene synthesis. *Science* **2023,** *381* (6660), 886-890.
46. Shi, X.; Cheng, D.; Zhao, R.; Zhang, G.; Wu, S.; Zhen, S.; Zhao, Z.-J.; Gong, J., Accessing complex reconstructed material structures with hybrid global optimization accelerated via on-the-fly machine learning. *Chem. Sci.* **2023,** *14* (33), 8777-8784.
47. Jeon, B.; Sankaranarayanan, S. K. R. S.; Ramanathan, S., Atomistic Modeling of Ultrathin Surface Oxide Growth on a Ternary Alloy: Oxidation of Al−Ni−Fe. *J. Phys. Chem. C* **2011,** *115* (14), 6571-6580.
48. Pollock, T. M.; Tin, S., Nickel-Based Superalloys for Advanced Turbine Engines: Chemistry, Microstructure and Properties. *J. Propuls. Power* **2006,** *22* (2), 361-374.
49. Anklekar, R. M.; Bauer, K.; Agrawal, D. K.; Roy, R., Improved mechanical properties and microstructural development of microwave sintered copper and nickel steel PM parts. *Powder Metall.* **2005,** *48* (1), 39-46.
50. Darken, L. S.; Gurry, H. W., *Physical Chemistry of Metals*. McGraw-Hill: New York, NY, 1953.
51. Islam, M. A., Einstein–Smoluchowski Diffusion Equation: A Discussion. *Phys. Scr.* **2004,** *70* (2-3), 120.

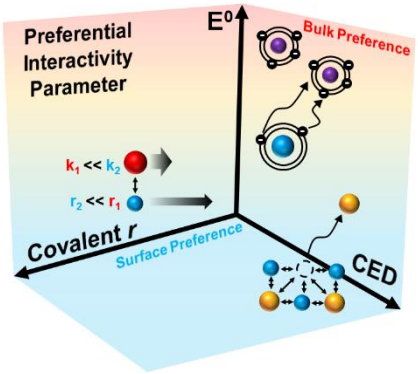

SYNOPSIS TOC Understanding oxidation is a critical element in metal alloy designs. Engineering resulting nanostructure(s) can provide unique opportunities for improving material properties. Herein, we introduce the thermodynamic-based preferential interactivity parameter and provide our perspective towards surface oxidation in multi-element systems whilst considering the higher dimensionality of underlying kinetics. We make a case why nano scientists need to pay attention to these oxides by pointing to fundamental and applied work that still needs to be done.